IEEE Access
Multidisciplinary ⋮ Rapid Review ⋮ Open Access Journal

Received 25 June 2022, accepted 17 July 2022, date of publication 21 July 2022, date of current version 27 July 2022.

Digital Object Identifier 10.1109/ACCESS.2022.3193255

RESEARCH ARTICLE

Anti-Disturbance Dynamic Surface Control for Air-Breathing Hypersonic Vehicles Based on NDO

OUXUN LI[1,2], JU JIANG[1], LI DENG[2], AND SHUTONG HUANG[1,2]
[1]College of Automation Engineering, Nanjing University of Aeronautics and Astronautics, Nanjing 211106, China
[2]School of Electronic Information and Automation, Guilin University of Aerospace Technology, Guilin 541004, China

Corresponding author: Ouxun Li (liouxun@guat.edu.cn)

This work was supported in part by the Natural Science Foundation of China under Grant 61966010, and in part by the Natural Science Foundation of Guangxi Province under Grant 2022GXNSFBA035508.

ABSTRACT This paper is concerned with the anti-disturbance dynamic surface controller (DSC) design for an air-breathing hypersonic vehicle (AHV) based on nonlinear disturbance observer (NDO). For the longitudinal model of AHV subjected to the high nonlinearity, the uncertain parameters and the varying disturbance, the feedback linearization method is employed considering the uncertain parameters. Then, a dynamic surface controller is designed based on the inverse hyperbolic sine function to solve the problem of "explosion of terms" in the traditional backstepping control. Furthermore, in order to enhance the disturbance rejection ability, a novel NDO is designed to estimate the model uncertainties and external disturbances. Finally, the simulation results verify the superior tracking performance of the proposed control strategy.

INDEX TERMS Air-breathing hypersonic vehicle, anti-disturbance, dynamic surface control, nonlinear disturbance observer.

I. INTRODUCTION

Air-breathing hypersonic vehicle (AHV) has become an important development trend in the global aerospace technology, considering the widespread applications both in military and civil areas [1]. However, compared with the traditional flight vehicles, AHV has the characteristics of strong nonlinearity, strong coupling, model uncertainty and sensitivity to external disturbance, which brings challenges for the flight control system design. For the control problem of model uncertainty and external disturbance, which includes unmodeled dynamics, structural elastic deformation, modeling error and random interference, the control method must have strong disturbance rejection ability [2], [3]. To further improve the control performance, the flight control of AHV has been widely explored such as the sliding mode control (SMC) [4], [5], the adaptive control [6]–[8], the robust control [9], the backstepping control [10]–[14], the intelligent control [15]–[20], etc.

The associate editor coordinating the review of this manuscript and approving it for publication was Haibin Sun.

The backstepping control method is one of the most effective methodologies for the tracking control of a large class of strict-feedback systems. It has been widely applied to many kinds of control plants such as the unmanned air vehicles (UAV), the quadrotor, the robot, the AHV, etc. In [11], authors present a command filtered backstepping approach to control the UAV, which includes the adaptive approximation of the aerodynamic force and moment coefficient functions. In [12], authors discuss the results of backstepping and sliding mode control techniques applied to the quadrotor. A combined kinematic/torque control law is developed using backstepping and stability is guaranteed by the Lyapunov theory for nonholonomic mobile robots [13]. A novel model transformation and a novel adaptive backstepping control method are proposed for AHV with uncertain parameters [14]. With the development of technology, scholars have proposed some improved backstepping control methods such as combination of backstepping control and intelligent control. A backstepping based control design for a class of nonlinear systems in strict-feedback form with arbitrary uncertainty by incorporating backstepping into a neural network based adaptive control design framework [15]. An adaptive fuzzy control

strategy is used to compensate the unknown nonlinearities and modeling errors caused by variable flight conditions [16]. In [17], authors proposed a nonsingular direct neural control of AHV via back-stepping, where the neural network is used to estimate the virtual and actual control laws derived from backstepping design. A new back-stepping control approach is proposed for AHV non-affine models via the neural approximation, and the robust adaptive tracking control laws are developed using improved back-stepping designs [19]. Recently, in order to guarantee the real-time performance, and reduce the structure and computation complexity, some scholars proposed backstepping-avoidance-based strategies. In [20], authors designed a new back-stepping control without virtual control laws for the altitude subsystem of the AHV via a model transformation combined with low-pass filter approach. In [21] and [22], in order to further reduce computational costs, authors presented a low-complexity design strategies without back-stepping for waverider vehicles via fuzzy-neural approximation. It can be seen that the intelligent control methods can improve the control performance but with high complexity, which is not conducive to online calculation and implementation.

It is well known that the dynamic surface control (DSC) is designed to solve the problem of ''explosion of terms'' in the traditional backstepping control by introducing the tracking differentiator (TD). In [23], a method is proposed by introducing a low pass filter for designing controllers with arbitrarily small tracking error for uncertain and mismatched nonlinear systems in the strict feedback form. A DSC technique combined with the Neural Network adaptive framework is presented to design a robust longitudinal dynamics controller for the AHV [24]. In [25], authors proposed a nonlinear adaptive dynamic surface air speed and a flight path angle control design procedure for the longitudinal dynamics of the AHV.

When backstepping is applied to AHV, for the convenience of controller design, the AHV model can be described as a kind of strict feedback nonlinear system based on the reasonable assumption. For the control problem of uncertainty and external disturbance, the disturbance observers can reduce the influences of the unknown uncertainties and disturbances, and enhance the robustness of the closed loop systems. In [26], authors present a general design method of new nonlinear disturbance observer (NDO) based on TD for uncertain dynamic systems. To enhance the controller's robustness, a new TD is designed based on hyperbolic sine function and a new NDO is constructed using the TD to estimate the model uncertainties and varying disturbances [27]. In [28], a fault-tolerant output tracking control method is proposed for AHV, and a disturbance observer is utilized to estimate the lumped effect of model uncertainties, external disturbances, and actuator faults. In [29], a disturbance observer based gain adaptation high-order sliding mode control method is proposed for AHV, where the observer is employed to estimate and reject the uncertainties and external disturbance.

In this paper, a novel robust backstepping approach for the longitudinal dynamical model of AHV is proposed. The contributions of this paper can be concluded as follows:

1) According to the nonlinear systems theory, the longitudinal dynamical model of AHV is described as a strict feedback nonlinear form with mismatched disturbances. Furthermore, the equations of the mismatching uncertainties terms are presented.

2) The Anti-disturbance dynamic surface controller based on NDO is designed for AHV with the uncertain parameters and the varying disturbance. Meanwhile, the block diagrams of the overall control scheme of the DSC and the NDO design are presented. Furthermore, the tuning guidelines of the control parameters are given.

3) In order to solve the problem of ''explosion of terms'', a new TD based on the inverse hyperbolic sine function is designed for each step of the virtual control laws. More specially, in order to enhance the robustness of system by estimating and compensating the model uncertainties and disturbances, a novel NDO based on the proposed TD is designed. The proposed NDO does not need any prior information of unknown disturbance, and has simple structure and few design parameters. Therefore, it has a certain application prospect.

4) The stabilities of the proposed TD, NDO and the closed-loop system are analyzed and proved based on the Lyapunov theory, respectively. Furthermore, the efficiency and robustness of the proposed control method are demonstrated by numerical simulations.

The remainder of this paper is organized as follows. In Section 2, the longitudinal dynamical model of AHV is described as a strict feedback nonlinear form with unmatched disturbances. Section 3 presents the design of DSC including a new TD based on the inverse hyperbolic sine function and a new NDO based on the proposed TD. The design method and the convergence of TD and NDO are discussed respectively, and the stability of the closed-loop system is also proved. The AHV case simulations and discussions are provided in Section 4, followed by the conclusion in Section 5.

II. PRELIMINARIES

A. AHV MODEL DESCRIPTION

AHV has extremely complex dynamic characteristics. In order to simplify the modeling problem without losing generality, the following assumptions could be made in the modeling process of AHV.

Assumption 1: The AHV is an ideal rigid body and the elastic degrees of freedom of wing, fuselage and tail are not considered in the modeling process.

Assumption 2: The influence of earth rotation on aircraft modeling is not considered, and the ground is assumed to be locally flat with constant gravitational acceleration.

Assumption 3: The geometric shape and internal mass distribution of AHV are symmetrical.

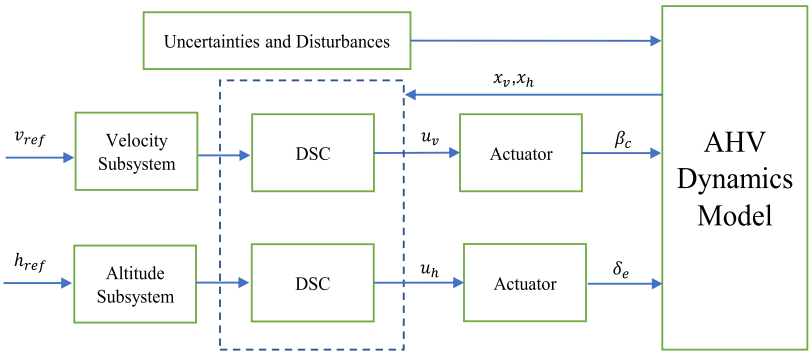

FIGURE 1. Block diagram of the DSC design.

Assumption 4: Ignoring the influence of asymmetry, compressibility and gust and other factors of air flow.

According to [14], [30], and [31], the nonlinear equations of the longitudinal motion are formulated as

$$\begin{cases} \dot{v} = \dfrac{T\cos\alpha - D}{m} - g\sin\gamma \\ \dot{\gamma} = \dfrac{L + T\sin\alpha}{mv} - \dfrac{(\mu - v^2 r)\cos\gamma}{vr^2} \\ \dot{q} = \dfrac{M_y}{I_y} \\ \dot{\alpha} = q - \dot{\gamma} \\ \dot{h} = v\sin\gamma \\ \ddot{\beta} = -2\xi\omega\dot{\beta} - \omega^2\beta + \omega^2\beta_c, \end{cases} \tag{1}$$

where v, γ, q, α, h are the flight velocity, the track angle, the pitch angle rate, the attack angle, the flight altitude, respectively; β_c, ω_n and ξ are the throttle setting, the engine natural frequency and the damp ratio, respectively. The parameters of the lift L, the drag D, the thrust T and the pitching moment M_y are given as follows

$$\begin{cases} L = \dfrac{1}{2}\rho v^2 s C_L \\ D = \dfrac{1}{2}\rho v^2 s C_D \\ T = \dfrac{1}{2}\rho v^2 s C_T \\ M_y = \dfrac{1}{2}\rho v^2 s\bar{c}(C_M^{\alpha} + C_M^{q} + C_M^{\delta_e}), \end{cases} \tag{2}$$

where $C_L, C_D, C_T, C_M^{\alpha}, C_M^{q}, C_M^{\delta_e}$ are coefficients for the lift, the drag, the thrust and the pitch moment, respectively. The curve-fitted approximations are expressed as

$$\begin{cases} C_L = C_L^{\alpha}\alpha \\ C_D = C_D^{\alpha^2}\alpha^2 + C_D^{\alpha}\alpha + C_D^0 \\ C_T = C_T^{\beta}\beta + C_T^0 \\ C_M^{\alpha} = C_M^{\alpha,\alpha^2}\alpha^2 + C_M^{\alpha,\alpha}\alpha + C_M^{\alpha,0} \\ C_M^{q} = C_M^{q,\alpha^2}\alpha^2 + C_M^{q,\alpha}\alpha + C_M^{q,0} \\ C_M^{\delta_e} = c_e(\delta_e - \alpha). \end{cases} \tag{3}$$

According to (2) and (3), one can get the functional relationships between the lift L, the drag D, the thrust T and the pitching moment M_y and variables of ρ, v, α, β and q.

$$\begin{cases} L = f_L(\rho, v, \alpha) \\ D = f_D(\rho, v, \alpha) \\ T = f_T(\rho, v, \alpha, \beta) \\ M_y = f_{M_y}(\rho, v, \alpha, q) + f_{\delta_e}\delta_e. \end{cases} \tag{4}$$

Considering all parameters of AHV are uncertain, they are expressed as $i = i_0(1 + \Delta i)$, $i = m, s, \bar{c}, c_e, I_{yy}, C_L^{\alpha}, C_D^{\alpha^2}, C_D^{\alpha}, C_D^0, C_T^{\beta}, C_T^0, C_M^{\alpha,\alpha^2}, C_M^{\alpha,\alpha}, C_M^{\alpha,0}, C_M^{q,\alpha^2}, C_M^{q,\alpha}, C_M^{q,0}$. where i represents the real value of parameter, i_0 denotes the nominal value, and Δi indicates the unknown constant. The state v in Equation (1) can be rewritten as

$$\begin{aligned} \dot{v} &= -g\sin\gamma + \frac{(T_0 + \Delta T)\cos\alpha - (D_0 + \Delta D)}{m_0 + \Delta m} \\ &= -g\sin\gamma \\ &\quad + \frac{\bar{q}(s_0 + \Delta s)((C_{T_0} + \Delta C_T)\cos\alpha - (C_{D_0} + \Delta C_D))}{m_0 + \Delta m} \\ &= -g\sin\gamma + \frac{T_0\cos\alpha - D_0}{m_0 + \Delta m} + \Delta v_{\lambda 1} + \Delta v_{\lambda 2} + \Delta v_{\lambda 3} \\ &= \dot{v}_0 + \Delta v_{\lambda} \end{aligned} \tag{5}$$

$$\begin{aligned} \dot{\gamma} &= \frac{-g\cos\gamma}{v} + \frac{(T_0 + \Delta T)\sin\alpha + (L_0 + \Delta L)}{(m_0 + \Delta m)v} \\ &= \frac{-g\cos\gamma}{v} \\ &\quad + \frac{\bar{q}(s_0 + \Delta s)((C_{T_0} + \Delta C_T)\sin\alpha + (C_{L_0} + \Delta C_L))}{(m_0 + \Delta m)v} \\ &= \frac{-g\cos\gamma}{v} + \frac{T_0\sin\alpha + L_0}{(m_0 + \Delta m)v} + \Delta\gamma_{\lambda 1} + \Delta\gamma_{\lambda 2} + \Delta\gamma_{\lambda 3} \\ &= \dot{\gamma}_0 + \Delta\gamma_{\lambda} \end{aligned} \tag{6}$$

$$\begin{aligned} \dot{q} &= \frac{\bar{q}(s_0 + \Delta s)(\bar{c}_0 + \Delta\bar{c})(C_{M0} + \Delta C_M)}{I_{yy0} + \Delta I_{yy}} \\ &= \frac{\bar{q}s_0\bar{c}_0(C_{M0}^{\alpha} + C_{M0}^{q} + C_{M0}^{\delta_e})}{I_{yy0} + \Delta I_{yy}} + \Delta q_{\lambda 1} + \Delta q_{\lambda 2} + \Delta q_{\lambda 3} \\ &= \dot{q}_0 + \Delta q_{\lambda} \end{aligned} \tag{7}$$

where,

$$\begin{cases} \bar{q} = 0.5\rho v^2 \\ \dot{v}_0 = -g sin\gamma + \dfrac{T_0 cos\alpha - D_0}{m_0 + \Delta m} \\ \dot{\gamma}_0 = \dfrac{-g cos\gamma}{v} + \dfrac{T_0 sin\alpha + L_0}{(m_0 + \Delta m)v} \\ \dot{q}_0 = \dfrac{\bar{q} s_0 \bar{c}_0 (C_{M0}^{\alpha} + C_{M0}^{q} + C_{M0}^{\delta_e})}{I_{yy0} + \Delta I_{yy}} \\ C_{M0} = C_{M0}^{\alpha} + C_{M0}^{q} + C_{M0}^{\delta_e} \\ \Delta C_M = \Delta C_M^{\alpha} + \Delta C_M^{q} + \Delta C_M^{\delta_e} \\ \Delta v_\lambda = \Delta v_{\lambda 1} + \Delta v_{\lambda 2} + \Delta v_{\lambda 3} \\ \Delta \gamma_\lambda = \Delta \gamma_{\lambda 1} + \Delta \gamma_{\lambda 2} + \Delta \gamma_{\lambda 3} \\ \Delta q_\lambda = \Delta q_{\lambda 1} + \Delta q_{\lambda 2} + \Delta q_{\lambda 3}, \end{cases} \tag{8}$$

$$\begin{cases} \Delta v_{\lambda 1} = \dfrac{\Delta T_{\lambda 1} cos\alpha - \Delta D_{\lambda 1}}{m_0 + \Delta m} \\ \Delta v_{\lambda 2} = \dfrac{\Delta T_{\lambda 2} cos\alpha - \Delta D_{\lambda 2}}{m_0 + \Delta m} \\ \Delta v_{\lambda 3} = \dfrac{\Delta T_{\lambda 3} cos\alpha - \Delta D_{\lambda 3}}{m_0 + \Delta m} \\ \Delta \gamma_{\lambda 1} = \dfrac{\Delta T_{\lambda 1} sin\alpha + \Delta L_{\lambda 1}}{(m_0 + \Delta m)v} \\ \Delta \gamma_{\lambda 2} = \dfrac{\Delta T_{\lambda 2} sin\alpha + \Delta L_{\lambda 2}}{(m_0 + \Delta m)v} \\ \Delta \gamma_{\lambda 3} = \dfrac{\Delta T_{\lambda 3} sin\alpha + \Delta L_{\lambda 3}}{(m_0 + \Delta m)v} \\ \Delta q_{\lambda 1} = \dfrac{\bar{q} s_0 \bar{c}_0 \Delta C_M}{I_{yy0} + \Delta I_{yy}} \\ \Delta q_{\lambda 2} = \dfrac{\bar{q}(s_0 \Delta \bar{c} + \Delta s \bar{c}_0 + \Delta s \Delta \bar{c}) C_{M0}}{I_{yy0} + \Delta I_{yy}} \\ \Delta q_{\lambda 3} = \dfrac{\bar{q}(s_0 \Delta \bar{c} + \Delta s \bar{c}_0 + \Delta s \Delta \bar{c}) \Delta C_M}{I_{yy0} + \Delta I_{yy}}, \end{cases} \tag{9}$$

$$\begin{cases} \Delta T_{\lambda 1} = \bar{q} s_0 \Delta C_T \\ \Delta T_{\lambda 2} = \bar{q} \Delta s C_{T_0} \\ \Delta T_{\lambda 3} = \bar{q} \Delta s \Delta C_T \\ \Delta T = \Delta T_{\lambda 1} + \Delta T_{\lambda 2} + \Delta T_{\lambda 3} \\ \Delta D_{\lambda 1} = \bar{q} s_0 \Delta C_D \\ \Delta D_{\lambda 2} = \bar{q} \Delta s C_{D_0} \\ \Delta D_{\lambda 3} = \bar{q} \Delta s \Delta C_D \\ \Delta D = \Delta D_{\lambda 1} + \Delta D_{\lambda 2} + \Delta D_{\lambda 3} \\ \Delta L_{\lambda 1} = \bar{q} s_0 \Delta C_L \\ \Delta L_{\lambda 2} = \bar{q} \Delta s C_{L_0} \\ \Delta L_{\lambda 3} = \bar{q} \Delta s \Delta C_L \\ \Delta L = \Delta L_{\lambda 1} + \Delta L_{\lambda 2} + \Delta L_{\lambda 3}, \end{cases} \tag{10}$$

$$\begin{cases} \Delta C_L = \Delta C_L^{\alpha} \alpha \\ \Delta C_T = \Delta C_T^{\beta} \beta + \Delta C_T^{0} \\ \Delta C_D = \Delta C_D^{\alpha^2} \alpha^2 + \Delta C_D^{\alpha} \alpha + \Delta C_D^{0} \\ \Delta C_M^{\alpha} = \Delta C_M^{\alpha, \alpha^2} \alpha^2 + \Delta C_M^{\alpha, \alpha} \alpha + \Delta C_M^{\alpha, 0} \\ \Delta C_M^{q} = \Delta C_M^{q, \alpha^2} \alpha^2 + \Delta C_M^{q, \alpha} \alpha + \Delta C_M^{q, 0}. \end{cases} \tag{11}$$

Define the state vector as $\mathbf{x} = [v, \gamma, q, \alpha, h]$, according to the nonlinear system theory and the concept of Lie derivative, one gets

$$\begin{cases} \dot{v} = \dot{v}_0 + \Delta v_\lambda = f_1(\mathbf{x}) + \Delta f_1(\mathbf{x}) \\ \ddot{v} = \dfrac{\partial (f_1(\mathbf{x}) + \Delta f_1(\mathbf{x}))}{\partial \mathbf{x}} \dot{\mathbf{x}} = \omega_1 \dot{\mathbf{x}} + \Delta \omega_1 \dot{\mathbf{x}} \\ \dddot{v} = \dot{\mathbf{x}}^{\mathrm{T}} \dfrac{\partial (\omega_1 + \Delta \omega_1)}{\partial \mathbf{x}} \dot{\mathbf{x}} + (\omega_1 + \Delta \omega_1) \ddot{\mathbf{x}} \\ = (\omega_1 + \Delta \omega_1) \ddot{\mathbf{x}} + \dot{\mathbf{x}}^{\mathrm{T}} (\omega_2 + \Delta \omega_2) \dot{\mathbf{x}}, \end{cases} \tag{12}$$

where $f_1(\mathbf{x}) = \dot{v}_0$, $\Delta f_1(\mathbf{x}) = \Delta v_\lambda$, $\omega_1 = \frac{\partial f_1(\mathbf{x})}{\partial \mathbf{x}}$, $\omega_2 = \frac{\partial \omega_1}{\partial \mathbf{x}}$, $\Delta \omega_1 = \frac{\partial \Delta f_1(\mathbf{x})}{\partial \mathbf{x}}$, $\Delta \omega_2 = \frac{\partial \Delta \omega_1}{\partial \mathbf{x}}$.

$$\begin{cases} \dot{h} = v \sin\gamma \\ \ddot{h} = \dot{v} \sin\gamma + v\dot{\gamma} \cos\gamma \\ \dddot{h} = \ddot{v} \sin\gamma + 2\dot{v}\dot{\gamma} \cos\gamma - v\dot{\gamma}^2 \sin\gamma + v\ddot{\gamma} \cos\gamma \\ h^{(4)} = \dddot{v} \sin\gamma + 3\ddot{v}\dot{\gamma} \cos\gamma - 3\dot{v}\gamma^2 \sin\gamma \\ + 3\dot{v}\ddot{\gamma} \cos\gamma - v\dot{\gamma}^3 \cos\gamma \\ - 3v\dot{\gamma}\ddot{\gamma} \sin\gamma + v\dddot{\gamma} \cos\gamma, \end{cases} \tag{13}$$

where the first, second, and third derivatives of γ are obtained according to (6) as

$$\begin{cases} \dot{\gamma} = \dot{\gamma}_0 + \Delta \gamma_\lambda = f_2(\mathbf{x}) + \Delta f_2(\mathbf{x}) \\ \ddot{\gamma} = \dfrac{\partial (f_2(\mathbf{x}) + \Delta f_2(\mathbf{x}))}{\partial \mathbf{x}} \dot{\mathbf{x}} = \pi_1 \dot{\mathbf{x}} + \Delta \pi_1 \dot{\mathbf{x}} \\ \dddot{\gamma} = \dot{\mathbf{x}}^{\mathrm{T}} \dfrac{\partial (\pi_1 + \Delta \pi_1)}{\partial \mathbf{x}} \dot{\mathbf{x}} + (\pi_1 + \Delta \pi_1) \ddot{\mathbf{x}} \\ = (\pi_1 + \Delta \pi_1) \ddot{\mathbf{x}} + \dot{\mathbf{x}}^{\mathrm{T}} (\pi_2 + \Delta \pi_2) \dot{\mathbf{x}}, \end{cases} \tag{14}$$

where $f_2(\mathbf{x}) = \dot{\gamma}_0$, $\Delta f_2(\mathbf{x}) = \Delta \gamma_\lambda$, $\pi_1 = \frac{\partial f_2(\mathbf{x})}{\partial \mathbf{x}}$, $\pi_2 = \frac{\partial \pi_1}{\partial x}$, $\Delta \pi_1 = \frac{\partial \Delta f_2(\mathbf{x})}{\partial \mathbf{x}}$, $\Delta \pi_2 = \frac{\partial \Delta \pi_1}{\partial \mathbf{x}}$.

According to (12), (13) and (14), the velocity channel and altitude channel in (1) can be re-described as

$$\begin{cases} \dot{v}_1 = v_2 + \Phi_{v_1} \\ \dot{v}_2 = v_3 + \Phi_{v_2} \\ \dot{v}_3 = F_v + \mathbf{B}_v \mathbf{U} + \Phi_{v_3} \\ \dot{h}_1 = h_2 = v sin\gamma \\ \dot{h}_2 = h_3 + \Phi_{h_2} \\ \dot{h}_3 = h_4 + \Phi_{h_3} \\ \dot{h}_4 = F_h + \mathbf{B}_h \mathbf{U} + \Phi_{h_4}, \end{cases} \tag{15}$$

where $\mathbf{B} = [\mathbf{B}_v, \mathbf{B}_h]^{\mathrm{T}} = [b_{11}, b_{12}; b_{21}, b_{22}]$; $\mathbf{U} = [\beta_c, \delta_e]^{\mathrm{T}}$ indicates the control inputs; $\Phi_{v_i}, i = (1, 2, 3)$ and $\Phi_{h_j}, j = (1, 2, 3, 4)$ indicate the mismatching uncertainties terms.

Combine (12) (13) and (14), one obtains

$$\begin{cases} F_v = \dfrac{\omega_1 \ddot{\mathbf{x}}_0 + \dot{\mathbf{x}}^{\mathrm{T}} \omega_2 \dot{\mathbf{x}}}{m_0 + \Delta m} \\ F_h = 3\ddot{v}\dot{\gamma}\cos\gamma - 3\dot{v}\gamma^2 \sin\gamma \\ + 3\dot{v}\ddot{\gamma}\cos\gamma - v\dot{\gamma}^3\cos\gamma \\ - 3v\dot{\gamma}\ddot{\gamma}\sin\gamma + \dfrac{(\omega_1 \ddot{\mathbf{x}}_0 + \dot{\mathbf{x}}^{\mathrm{T}} \omega_2 \dot{\mathbf{x}})\sin\gamma}{m_0 + \Delta m} \\ + v\cos\gamma(\pi_1 \ddot{\mathbf{x}}_0 + \dot{\mathbf{x}}^{\mathrm{T}} \pi_2 \dot{\mathbf{x}}) \\ b_{11} = \dfrac{\omega^2 \cos\alpha}{m_0 + \Delta m} \dfrac{\partial(T + \Delta T)}{\partial \beta} \\ b_{12} = \dfrac{\rho v^2 (s_0 + \Delta s)(\bar{c}_0 + \Delta \bar{c})(c_{e0} + \Delta c_e)}{2(m_0 + \Delta m)(I_{yy0} + \Delta I_{yy})} \\ (\dfrac{\partial(T + \Delta T)}{\partial \alpha} - (T + \Delta T)\sin\alpha - \dfrac{\partial(D + \Delta D)}{\partial \alpha}) \\ b_{21} = \dfrac{\omega^2 \sin(\alpha + \gamma)}{m_0 + \Delta m} \dfrac{\partial(T + \Delta T)}{\partial \beta} \\ b_{22} = \dfrac{\rho v^2 (s_0 + \Delta s)(\bar{c}_0 + \Delta \bar{c})(c_{e0} + \Delta c_e)}{2(m_0 + \Delta m)(I_{yy0} + \Delta I_{yy})} \\ (\dfrac{\partial(T + \Delta T)}{\partial \alpha}\sin(\alpha + \gamma) \\ + (T + \Delta T)\cos(\alpha + \gamma) \\ + \dfrac{\partial(L + \Delta L)}{\partial \alpha}\cos\gamma - \dfrac{\partial(D + \Delta D)}{\partial \alpha}\sin\gamma), \end{cases} \tag{16}$$

$$\begin{cases} \Phi_{v_1} = \Delta f_1 \\ \Phi_{v_2} = \Delta\omega_1 \dot{\mathbf{x}} \\ \Phi_{v_3} = \Delta\omega_1 \ddot{\mathbf{x}}_0 + \dot{\mathbf{x}}^{\mathrm{T}} \Delta\omega_2 \dot{\mathbf{x}} \\ \Phi_{h_2} = \Delta f_1 sin\gamma + v\Delta f_2 cos\gamma \\ \Phi_{h_3} = \Delta\omega_1 \dot{\mathbf{x}} sin\gamma - v(2f_2\Delta f_2 + \Delta f_2^2) sin\gamma \\ + 2(f_1\Delta f_2 + \Delta f_1 f_2 + \Delta f_1\Delta f_2) cos\gamma \\ + v\Delta\pi_1 \dot{\mathbf{x}} cos\gamma \\ \Phi_{h_4} = 3(\omega_1 \dot{\mathbf{x}}\Delta f_2 + \Delta\omega_1 \dot{\mathbf{x}} f_2 + \Delta\omega_1 \dot{\mathbf{x}}\Delta f_2) cos\gamma \\ - v(3f_2\Delta f_2^2 + 3f_2^2\Delta f_2 + \Delta f_2^3) cos\gamma \\ + 3(\pi_1 \dot{\mathbf{x}}\Delta f_1 + \Delta\pi_1 \dot{\mathbf{x}} f_1 + \Delta\pi_1 \dot{\mathbf{x}}\Delta f_1) cos\gamma \\ - 3v(\pi_1 \dot{\mathbf{x}}\Delta f_2 + \Delta\pi_1 \dot{\mathbf{x}} f_2 + \Delta\pi_1 \dot{\mathbf{x}}\Delta f_2) sin\gamma \\ + v(\Delta\pi_1 \ddot{\mathbf{x}}_0 + \dot{\mathbf{x}}^{\mathrm{T}} \Delta\pi_2 \dot{\mathbf{x}}) cos\gamma - 3\Delta f_1 \gamma^2 sin\gamma \\ + (\Delta\omega_1 \ddot{\mathbf{x}}_0 + \dot{\mathbf{x}}^{\mathrm{T}} \Delta\omega_2 \dot{\mathbf{x}}) sin\gamma, \end{cases} \tag{17}$$

where the function $f_1(\mathbf{x})$ and $f_2(\mathbf{x})$ are removed in brief.

III. CONTROLLER DESIGN

The equations of motion are decomposed into velocity subsystem and altitude subsystem. The block diagram of the overall control scheme of the DSC design is shown in Fig. 1 and Fig. 2. The controller uses the following parameters to control the AHV, including the signals from reference trajectories v_{ref} and h_{ref}, system states x_v and x_h, the estimates of the NDO $\hat{v}$, $\dot{\hat{v}}$, $\ddot{\hat{v}}$, $\hat{h}$, $\dot{\hat{h}}$, $\ddot{\hat{h}}$, $\dddot{\hat{h}}$, $\hat{d}_{v_i}(i = 1, 2, 3)$, and $\hat{d}_{h_j}(j = 1, 2, 3, 4)$, the virtual control law z_{v_1}, z_{v_2}, z_{h_1}, z_{h_2}, and z_{h_3}, the actual control law u_v and u_h, the throttle setting β_c and the elevator deflection δ_e.

A. TRACKING DIFFERENTIATOR DESIGN

The anti-hyperbolic sine function is smooth and continuous, which can eliminate the high-frequency flutter phenomenon. The tracking differentiator based on the anti-hyperbolic sine function can be described as

$$\begin{cases} \dot{x}_1(t) = x_2(t) \\ \dot{x}_2(t) = -\Gamma^2 a_1 \Theta(b_1(x_1(t) - r(t))) \\ - \Gamma^2 a_2 \Theta(b_2 x_2(t)/\Gamma), \end{cases} \tag{18}$$

where $\Theta(\cdot) = arsh(\cdot)$ represents the anti-hyperbolic sine function; $x_1(t)$ and $x_2(t)$ are the system states; $r(t)$ is the input signal; $\Gamma > 0, a_i > 0, b_i > 0, i = (1, 2)$ are the system design parameters.

Theorem 1: Consider the following second-order system

$$\begin{cases} \dot{\varepsilon}_1(t) = \varepsilon_2(t) \\ \dot{\varepsilon}_2(t) = g(\varepsilon_1(t), \varepsilon_2(t)), \end{cases} \tag{19}$$

if the solutions of the system (19) satisfy $\lim_{t\to\infty} \varepsilon_1(t) = 0$ and $\lim_{t\to\infty} \varepsilon_2(t) = 0$, for any arbitrarily bounded and integrable function $r(t)$, the solution of the following system

$$\begin{cases} \dot{z}_1(t) = z_2(t) \\ \dot{z}_2(t) = \Gamma^2 g((z_1(t) - r(t)), z_2(t)/\Gamma)), (\Gamma > 0), \end{cases} \tag{20}$$

satisfies

$$\lim_{\Gamma\to\infty} \int_0^T |\varepsilon_1(t) - r(t)| dt = 0, \quad (T > 0). \tag{21}$$

Proof: Define a Lyapunov function as follow

$$\begin{aligned} L(\varepsilon_1(t), \varepsilon_2(t)) &= \int_0^{\varepsilon_1(t)} a_1 \Theta(b_1 \tau) d\tau + 0.5\varepsilon_2^2(t) \\ &= a_1 \varepsilon_1(t) \Theta(b_1 \delta) + 0.5\varepsilon_2^2(t), (0 < \delta < \varepsilon_1(t)). \end{aligned} \tag{22}$$

Since $\Theta(\cdot)$ is an odd function, if $a_1 > 0$, $b_1 > 0$, $\varepsilon_1(t) > 0$, one has $a_1\varepsilon_1(t)\Theta(b_1\delta) > 0$, then $L(\varepsilon_1(t), \varepsilon_2(t)) > 0$.

Define $g(\varepsilon_1(t), \varepsilon_2(t)) = -a_1\Theta(b_1\varepsilon_1(t)) - a_2\Theta(b_2\varepsilon_2(t))$. Taking the time derivation of $L(\varepsilon_1(t), \varepsilon_2(t))$, if $a_2 > 0$, $b_2 > 0$, one gets

$$\begin{aligned} \dot{L}(\varepsilon_1(t), \varepsilon_2(t)) &= a_1 \dot{\varepsilon}_1(t) \Theta(b_1 \varepsilon_1(t)) + \varepsilon_2(t) \dot{\varepsilon}_2(t) \\ &= a_1 \varepsilon_2(t) \Theta(b_1 \varepsilon_1(t)) \\ &\quad + \varepsilon_2(-a_1 \Theta(b_1 \varepsilon_1(t)) - a_2 \Theta(b_2 \varepsilon_2(t))) \\ &= -a_2 \varepsilon_2 \Theta(b_2 \varepsilon_2(t)) \le 0. \end{aligned} \tag{23}$$

It can be seen from (23) that only when $\varepsilon_2(t) = 0$, $\dot{L}(\varepsilon_1(t), \varepsilon_2(t)) = 0$. When $\dot{L}(\varepsilon_1(t), \varepsilon_2(t)) = 0$, if $\varepsilon_1(t) \neq 0$, then $\dot{\varepsilon}_2(t) \neq 0$ according to (19). That is, $\varepsilon_2(t) = 0$ is instable if $\varepsilon_1(t) \neq 0$. Through the above analysis, it can be concluded that if and only if $\varepsilon_1(t) = \varepsilon_2(t) = 0$, $\dot{L}(\varepsilon_1(t), \varepsilon_2(t)) = 0$. Therefore, according to the Lyapunov theorem, the system (20) is asymptotically stable at the origin $(0, 0)$. Moreover, when Γ is big enough, the solution $x_1(t)$ of the system (18) can fully approach the input signal $r(t)$, it means that $\dot{x}_1(t) = x_2(t) = \dot{r}(t)$. This is the end of the proof. ■

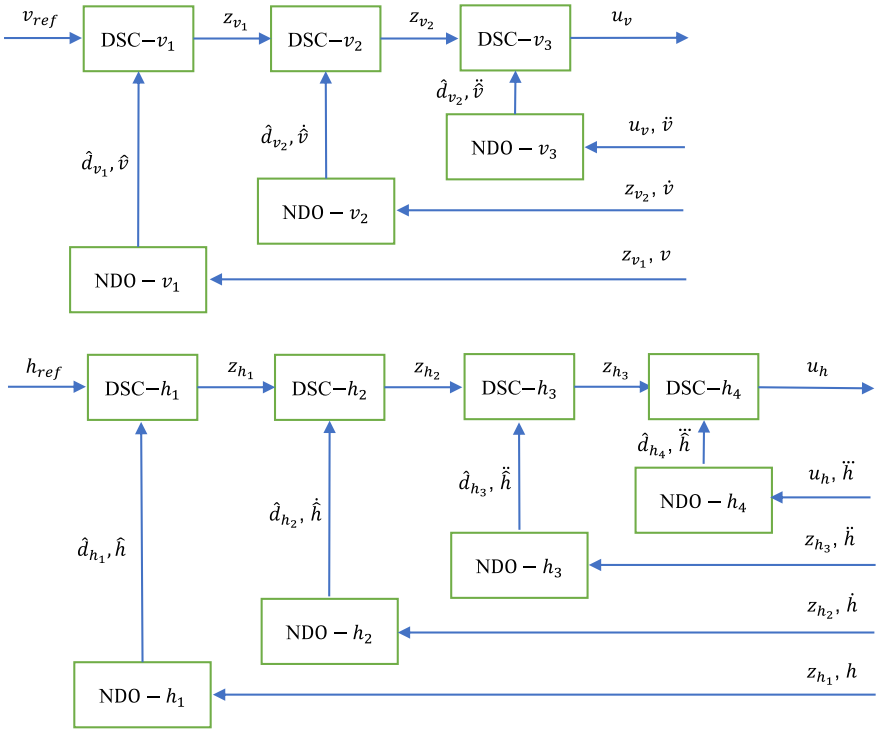

FIGURE 2. Block diagram of the NDO design.

B. NONLINEAR DISTURBANCE OBSERVER DESIGN

Consider the following uncertain system

$$\dot{z} = \phi(z) + \eta(z)u + d \tag{24}$$

where $\phi(z)$ and $\eta(z)$ are given functions, d denotes the system disturbance. A new NDO can be expressed as

$$\begin{cases} \dot{\hat{z}} = \phi(z) + \eta(z)u + \hat{d} \\ \dot{\hat{d}} = -\Gamma^2(a_1\Theta(b_1(\hat{z} - z)) + a_2\Theta(b_2\hat{d}/\Gamma)), \end{cases} \tag{25}$$

where $\Theta(\cdot) = arsh(\cdot)$ represents the anti-hyperbolic sine function, $\hat{z}$ and $\hat{d}$ represent the respective estimations of z and d, $\Gamma > 0$, $a_i > 0$, $b_i > 0$, $i = (1, 2)$ are the system design parameters.

Theorem 2: consider the following system

$$\begin{cases} \dot{\hat{z}} = \phi(z) + \eta(z)u + \hat{d} \\ \dot{\hat{d}} = \Gamma^2\Xi(\hat{z} - z, \hat{d}/\Gamma), \end{cases} \tag{26}$$

if the system design parameter $\Gamma > 0$, one gets

$$\lim_{\Gamma\to\infty} \int_0^T |\hat{z} - z| dt = 0, \quad (T > 0). \tag{27}$$

Furthermore,

$$\begin{cases} \hat{z} \to z \\ \hat{d} \to d. \end{cases} \tag{28}$$

Proof: When the system design parameter $\Gamma \to \infty$ in the equation (26), one gets

$$|\dot{\hat{d}}| = |\Gamma^2\Xi(\hat{z} - z, \hat{d}/\Gamma)| \to \infty. \tag{29}$$

It can be seen from the equation (29) that $\hat{d}$ varies much faster than $\phi(z) + \eta(z)u$ when $\Gamma \to \infty$. According to the equation (26), we have

$$\begin{cases} \lim\limits_{\Gamma\to\infty} \dfrac{d(\phi(z) + \eta(z)u + \hat{d})}{dt} = \dot{\hat{d}} \\ \lim\limits_{\Gamma\to\infty} \dfrac{\phi(z) + \eta(z)u + \hat{d}}{\Gamma} = \dfrac{\hat{d}}{\Gamma}, \end{cases} \tag{30}$$

then we take $\phi(z) + \eta(z)u + \hat{d}$ as z_2, the equation (26) can be expressed as

$$\begin{cases} \dot{\hat{z}}_1 = z_2 \\ \dot{\hat{z}}_2 = \Gamma^2\Xi(\hat{z} - z, \hat{d}/\Gamma). \end{cases} \tag{31}$$

Thus according to Theorem 1, it is tempting to conclude that the Theorem 2 holds. This is the end of the proof. ■

It is worthy to point out that the characteristics of the NDO are determined by TD. Due to disturbance is the input signal of TD essentially, according to the requirements of TD for input signal, the proposed NDO does not need the prior information of disturbance.

C. DYNAMIC SURFACE CONTROLLER DESIGN

According to the velocity subsystem (15), consider the following nonlinear system

$$\begin{cases} \dot{v}_1 = v_2 + \Phi_{v_1} + d_{v_1} \\ \dot{v}_2 = v_3 + \Phi_{v_2} + d_{v_2} \\ \dot{v}_3 = F_v + B_v u_v + \Phi_{v_3} + d_{v_3}, \end{cases} \tag{32}$$

where, v_i, $i = (1, 2, 3)$ and u_v represent the states and control input, respectively. Φ_{vi}, $i = (1, 2, 3)$ and F_v are given functions. d_i, $i = (1, 2, 3)$ denotes the system disturbance.

Define the tracking errors of v_1,v_2,v_3 as follows

$$\begin{cases} e_{v_1} = v_1 - v_{ref} \\ e_{v_2} = v_2 - z_{v_1} \\ e_{v_3} = v_3 - z_{v_2}. \end{cases} \tag{33}$$

Based on the backstepping and dynamic inversion theory, the virtual control law z_{v_1}, z_{v_2} and the actual control law u_v are chosen as

$$\begin{cases} z_{v_1} = -k_{v_1,1}e_{v_1} - k_{v_1,2}\int_0^t e_{v_1}(\tau)d\tau - \Phi_{v_1} - \hat{d}_{v_1} + \dot{v}_{ref} \\ z_{v_2} = -k_{v_2,1}e_{v_2} - k_{v_2,2}\int_0^t e_{v_2}(\tau)d\tau - \Phi_{v_2} - \hat{d}_{v_2} \\ + \dot{\hat{z}}_{v_1} - e_{v_1} \\ u_v = B_v^{-1}(-k_{v_3,1}e_{v_3} - k_{v_3,2}\int_0^t e_{v_3}(\tau)d\tau - \Phi_{v_3} - \hat{d}_{v_3} \\ - F_v + \dot{\hat{z}}_{v_2} - e_{v_2}), \end{cases} \tag{34}$$

where $k_{i,1} > 0$, $k_{i,2} > 0$, $k_{i,3} > 0$ $(i = v_1, v_2)$ are design parameters. $\hat{d}_{v_1}$, $\hat{d}_{v_2}$ and $\hat{d}_{v_3}$ are the respective estimations of d_{v_1}, d_{v_2} and d_{v_3}. $\dot{z}_{v_1}$ and $\dot{z}_{v_2}$ are the respective derivatives of virtual control law z_{v_1}, z_{v_2}, $\dot{\hat{z}}_{v_1}$ and $\dot{\hat{z}}_{v_2}$ are the respective estimations of $\dot{z}_{v_1}$ and $\dot{z}_{v_2}$. According to the equation (18) $\dot{\hat{z}}_{v_1}$, $\dot{\hat{z}}_{v_2}$, d_{v_1}, d_{v_2} and d_{v_3} can be express as

$$\begin{cases} \dot{\hat{z}}_{v_1} = \omega_{v_1} \\ \dot{\omega}_{v_1} = -\Gamma_1^2(a_{11}\Theta(b_{11}(\hat{z}_{v_1} - z_{v_1}) + a_{12}\Theta(b_{12}\omega_{v_1}/\Gamma_1)) \\ \dot{\hat{z}}_{v_2} = \omega_{v_2} \\ \dot{\omega}_{v_2} = -\Gamma_2^2(a_{21}\Theta(b_{21}(\hat{z}_{v_2} - z_{v_2}) + a_{22}\Theta(b_{22}\omega_{v_2}/\Gamma_2)) \\ \dot{\hat{v}}_1 = v_2 + \Phi_{v_1} + \hat{d}_{v_1} \\ \dot{\hat{d}}_{v_1} = -\Gamma_3^2(a_{31}\Theta(b_{31}(\hat{v} - v_1) + a_{32}\Theta(b_{32}\hat{d}_{v_1}/\Gamma_3)) \\ \dot{\hat{v}}_2 = v_3 + \Phi_{v_2} + \hat{d}_{v_2} \\ \dot{\hat{d}}_{v_2} = -\Gamma_4^2(a_{41}\Theta(b_{41}(\hat{v}_2 - v_2) + a_{42}\Theta(b_{42}\hat{d}_{v_2}/\Gamma_4)) \\ \dot{\hat{v}}_3 = F_v + B_v u_v + \Phi_{v_3} + \hat{d}_{v_3} \\ \dot{\hat{d}}_{v_3} = -\Gamma_5^2(a_{51}\Theta(b_{51}(\hat{v}_3 - v_3) + a_{52}\Theta(b_{52}\hat{d}_{v_3}/\Gamma_5)). \end{cases} \tag{35}$$

Theorem 3: The closed-loop system (32), the virtual control laws and the actual control law (34), and the NDOs (35) guaranteed to have all the signals in the closed-loop system are semi-globally uniformly bounded.

Proof: The Lyapunov function is chosen as

$$\begin{cases} L_1 = \frac{1}{2}e_{v_1}^2 + \frac{1}{2}k_{v_1,2}(\int_0^t e_{v_1}(\tau)d\tau)^2 \\ L_2 = L_1 + \frac{1}{2}e_{v_2}^2 + \frac{1}{2}k_{v_2,2}(\int_0^t e_{v_2}(\tau)d\tau)^2 \\ L_3 = L_2 + \frac{1}{2}e_{v_3}^2 + \frac{1}{2}k_{v_3,2}(\int_0^t e_{v_3}(\tau)d\tau)^2. \end{cases} \tag{36}$$

Define the estimation errors of disturbances as $e_{d_1} = d_1 - \hat{d}_1$, $e_{d_2} = d_2 - \hat{d}_2$, and $e_{d_3} = d_3 - \hat{d}_3$. According to Theorem 3, taking the derivative of (36) and combining (33) and (34), we have

$$\begin{cases} \dot{L}_1 = -k_{v_1,1}e_{v_1}^2 + e_{v_1}e_{v_2} + e_{v_1}e_{d_1} \\ \dot{L}_2 = -k_{v_1,1}e_{v_1}^2 - k_{v_2,1}e_{v_2}^2 + e_{v_2}e_{v_3} + e_{v_1}e_{d_1} + e_{v_2}e_{d_2} \\ \dot{L}_3 = -k_{v_1,1}e_{v_1}^2 - k_{v_2,1}e_{v_2}^2 - k_{v_3,1}e_{v_3}^2 \\ + e_{v_1}e_{d_1} + e_{v_2}e_{d_2} + e_{v_3}e_{d_3}. \end{cases} \tag{37}$$

Consider the following inequality holds

$$\begin{cases} e_{v_1}e_{d_1} \le \dfrac{(e_{v_1}e_{d_1})^2 + 1}{2} \\ e_{v_2}e_{d_2} \le \dfrac{(e_{v_2}e_{d_2})^2 + 1}{2} \\ e_{v_3}e_{d_3} \le \dfrac{(e_{v_3}e_{d_3})^2 + 1}{2}, \end{cases} \tag{38}$$

$\dot{L}_3$ can be expressed as

$$\begin{aligned} \dot{L}_3 \le & -k_{v_1,1}e_{v_1}^2 - k_{v_2,1}e_{v_2}^2 - k_{v_3,1}e_{v_3}^2 \\ & + \frac{1}{2}(e_{v_1}e_{d_1})^2 + \frac{1}{2}(e_{v_2}e_{d_2})^2 + \frac{1}{2}(e_{v_3}e_{d_3})^2 + 1.5 \\ = & -(k_{v_1,1} - \frac{1}{2}e_{d_1}^2)e_{v_1}^2 - (k_{v_2,1} - \frac{1}{2}e_{d_2}^2)e_{v_2}^2 \\ & - (k_{v_3,1} - \frac{1}{2}e_{d_3}^2)e_{v_3}^2 + 1.5. \end{aligned} \tag{39}$$

Define $k_{v_1,1} > \frac{1}{2}e_{d_1}^2 + \delta$, $k_{v_2,1} > \frac{1}{2}e_{d_2}^2 + \delta$ and $k_{v_3,1} > \frac{1}{2}e_{d_3}^2 + \delta$, one gets

$$\begin{aligned} \dot{L}_3 & \le -\delta e_{v_1}^2 - \delta e_{v_2}^2 - \delta e_{v_3}^2 + 1.5 \\ & = -2\delta(\frac{1}{2}e_{v_1}^2 + \frac{1}{2}e_{v_2}^2 + \frac{1}{2}e_{v_3}^2) + 1.5 \\ & \le -2\delta L_3 + 1.5, \end{aligned} \tag{40}$$

when $\delta \ge \frac{1.5}{2L_3}$, one has $\dot{L}_3 \le 0$. Consequently, one can obtain that

$$L_3(t) \le \frac{0.75}{\delta} + (L_3(0) - \frac{0.75}{\delta})e^{2\delta t}. \tag{41}$$

By choosing appropriate design parameters $k_{v_i,1}(i = 1, 2, 3)$, the system tracking errors can be sufficient small. The proof is completed. ■

Similarly, according to the altitude subsystem (15), one has

$$\begin{cases} \dot{h}_1 = h_2 \\ \dot{h}_2 = h_3 + \Phi_{h_2} + d_{h_2} \\ \dot{h}_3 = h_4 + \Phi_{h_3} + d_{h_3} \\ \dot{h}_4 = F_h + B_h u_h + \Phi_{h_4} + d_{h_4}. \end{cases} \tag{42}$$

Define the tracking errors of h_1, h_2, h_3, and h_4, respectively as

$$\begin{cases} e_{h_1} = h_1 - h_{ref} \\ e_{h_2} = h_2 - z_{h_1} \\ e_{h_3} = h_3 - z_{h_2} \\ e_{h_4} = h_4 - z_{h_3}. \end{cases} \tag{43}$$

The virtual control laws $z_{h_1}, z_{h_2}, z_{h_3}$ and the actual control u_h are chosen as

$$\begin{cases} z_{h_1} = -k_{h_1,1}e_{h_1} - k_{h_1,2}\int_0^t e_{h_1}(\tau)d\tau - \hat{d}_{h_1} + \dot{v}_{ref} \\ z_{h_2} = -k_{h_2,1}e_{h_2} - k_{h_2,2}\int_0^t e_{h_2}(\tau)d\tau - \Phi_{h_2} - \hat{d}_{h_2} \\ + \dot{\hat{z}}_{h_1} - e_{h_1} \\ z_{h_3} = -k_{h_3,1}e_{h_3} - k_{h_3,2}\int_0^t e_{h_3}(\tau)d\tau - \Phi_{h_3} - \hat{d}_{h_3} \\ + \dot{\hat{z}}_{h_2} - e_{h_2} \\ u_h = B_h^{-1}(-k_{h_4,1}e_{h_4} - k_{h_4,2}\int_0^t e_{h_4}(\tau)d\tau - \Phi_{h_4} - \hat{d}_{h_4} \\ - F_h + \dot{\hat{z}}_{h_3} - e_{h_3}), \end{cases} \tag{44}$$

where $k_{i,1} > 0$, $k_{i,2} > 0$, $k_{i,3} > 0$ $(i = h_1, h_2, h_3)$ are design parameters. $\hat{d}_{h_1}, \hat{d}_{h_2}, \hat{d}_{h_3}$ and $\hat{d}_{h_4}$ are the corresponding estimations of $d_{h_1}, d_{h_2}, d_{h_3}$ and d_{h_4}.

It is worth noting that there is a coupling phenomenon between the velocity channel and the altitude channel, so the actual control signals for the throttle setting and the elevator deflection need to be decoupled. It means that the matrix $\mathbf{B} = [b_{11}, b_{12}; b_{21}, b_{22}]$ must satisfy nonsingular. It is reasonable to assume that the matrix $\mathbf{B}$ is nonsingular because the flight path angle of the AHV satisfies $\gamma \neq \pm\frac{\pi}{2}$ in the whole flight envelope.

IV. SIMULATIONS AND DISCUSSION

In this section, the numerical simulations are executed to validate the efficiency and robustness of the proposed control method, the mathematical model of the AHV is built on the MATLAB/Simulink platform, and the designed controller is also simulated and verified with MATLAB.

At the initial condition, Table 1 lists the initial flight condition and the uncertainty boundary. The external disturbances are given in Table 2. The control input constraints used in the AHV are shown in Table 3. The reference trajectories of velocity and altitude are set as step signal and are generated via the following filter:

$$\begin{cases} \dfrac{v_c(s)}{v_{ref}(s)} = \dfrac{0.005}{s^2 + 0.15s + 0.005} \\ \dfrac{h_c(s)}{h_{ref}(s)} = \dfrac{0.005}{s^2 + 0.15s + 0.005}, \end{cases} \tag{45}$$

where v_{ref} (s) and h_{ref} (s) represent the step signals of 50 (m/s) and 50 (m), respectively. The parameters adopted for control inputs are given in Table 4. Furthermore, the tuning guidelines of the control parameters are presented as follows.

1) Increasing Γ can improve the TD response speed, tracking and differential accuracy, but it will reduce the noise suppression ability. Too large Γ will lead to tracking and differential output flutter.

TABLE 1. Initial flight condition and uncertainty boundary.

State	Value	Parameters	Value	Boundary
v (m/s)	4590	m (kg)	50200	$\lvert\Delta m\rvert \leq 15\%$
h (m)	33528	I_{yy} (kg$\cdot$ m^2)	8466900	$\lvert\Delta I_{yy}\rvert \leq 15\%$
γ (rad)	0	s (m^2)	369	$\lvert\Delta s\rvert \leq 15\%$
α (rad)	0	$\bar{c}$ (m)	28	$\lvert\Delta\bar{c}\rvert \leq 15\%$
q (rad/s)	0	c_e	0.0292	$\lvert\Delta c_e\rvert \leq 15\%$

TABLE 2. External disturbances of the AHV.

Disturbance	Value
$d_{v_1}(t)$	$0.02\sin(0.04t)$
$d_{v_2}(t)$	$0.04\cos(0.02t)$
$d_{v_3}(t)$	$0.02\sin(0.04t) + 0.04\cos(0.02t)$
$d_{h_1}(t)$	$0.04\sin(0.02t)$
$d_{h_2}(t)$	$0.02\cos(0.04t)$
$d_{h_3}(t)$	$0.04\sin(0.02t) + 0.02\cos(0.04t)$
$d_{h_4}(t)$	$0.02\sin(0.04t) + 0.04\sin(0.02t)$

TABLE 3. Control input constraints of the AHV.

Control Input	Lower Bound	Upper Bound
β_c	0	1
δ_e (rad)	-0.52	0.52

TABLE 4. Parameters of the controller.

Controller	Value
z_{v_1}	$\Gamma_{v_1} = 0.005, k_{v_1,1} = 0.5, k_{v_1,2} = 0.05$ $a_{v_1,1} = a_{v_1,2} = 3, b_{v_1,1} = b_{v_1,2} = 1$
z_{v_2}	$\Gamma_{v_2} = 50, k_{v_2,1} = 1.5, k_{v_2,2} = 0.1$ $a_{v_2,1} = a_{v_2,2} = 3, b_{v_2,1} = b_{v_2,2} = 1$
u_v	$k_{v_3,1} = 2.5, k_{v_3,2} = 0.5$
z_{h_1}	$\Gamma_{h_1} = 0.005, k_{h_1,1} = 0.5, k_{h_1,2} = 0.05$ $a_{h_1,1} = a_{h_1,2} = 3, b_{h_1,1} = b_{h_1,2} = 1$
z_{h_2}	$\Gamma_{h_2} = 0.5, k_{h_2,1} = 1.5, k_{h_2,2} = 0.1$ $a_{h_2,1} = a_{h_2,2} = 3, b_{h_2,1} = b_{h_2,2} = 1$
z_{h_3}	$\Gamma_{h_3} = 50, k_{h_3,1} = 2, k_{h_3,2} = 0.3$ $a_{h_3,1} = a_{h_3,2} = 3, b_{h_3,1} = b_{h_3,2} = 1$
u_h	$k_{h_4,1} = 2.5, k_{h_4,2} = 0.5$

2) a_1 is similarly to Γ. a_2 has a great influence on the differential effect. Increasing a_2 can improve the noise suppression ability, but will reduce the response speed

3) Increasing b can improve the noise suppression ability, but too lager value will increase the tracking error.

4) According to the control system structure and the backstepping control theory, in order to achieve better control effect, it is necessary to satisfy the response speed of the inner loop is faster than that of the outer loop. Thus, the parameters can be designed as $\Gamma_{v_2} > \Gamma_{v_1}, k_{v_3} > k_{v_2} > k_{v_1}$, $\Gamma_{h_3} > \Gamma_{h_2} > \Gamma_{h_1}, k_{h_4} > k_{h_3} > k_{h_2} > k_{h_1}$.

In order to demonstrate the efficiency of the proposed method, 5% to 15% parameter uncertainties and external disturbances are considered. The simulation results are given in Figs. 3–19. In these pictures, Λ_{ref} represents the reference value of Λ, $est - \Lambda$ represents the estimation value of Λ, and $err - \Lambda$ represents the estimation error of Λ. dv and dh are the respective derivatives of velocity and altitude. z_{v_i} $(i = 1, 2)$ and z_{h_j} $(j = 1, 2, 3)$ represent the virtual control law

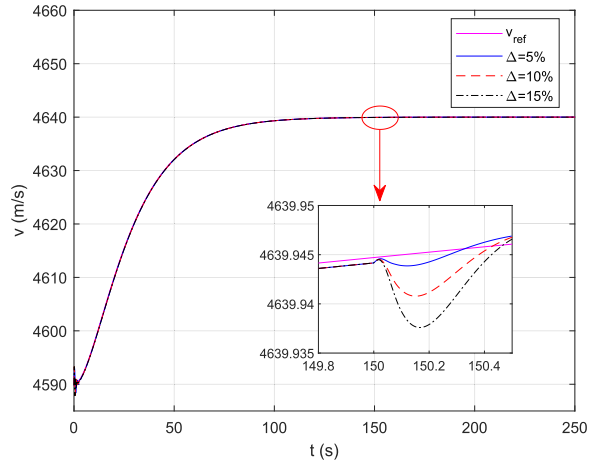

FIGURE 3. Responses of the velocity.

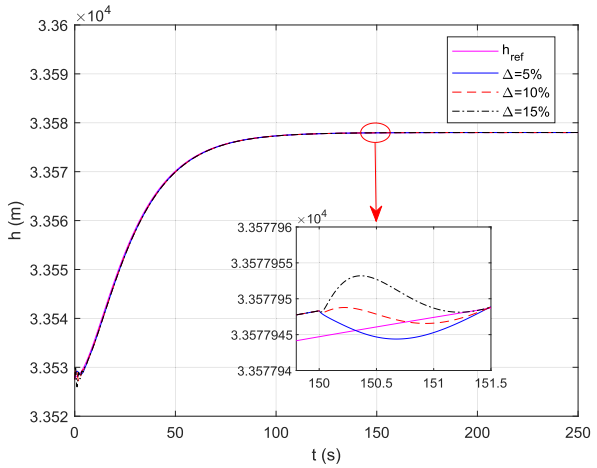

FIGURE 4. Responses of the altitude.

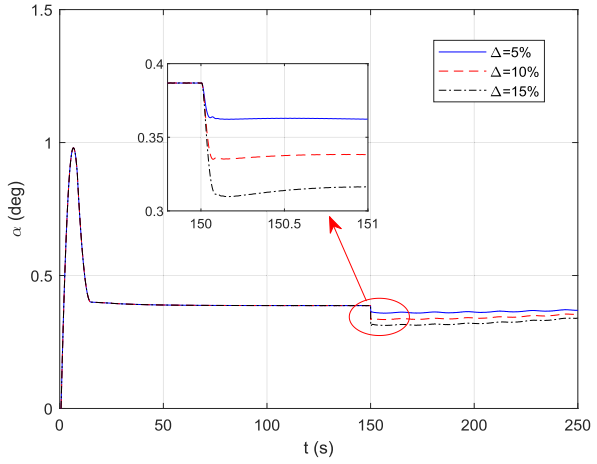

FIGURE 5. Responses of the attack angle.

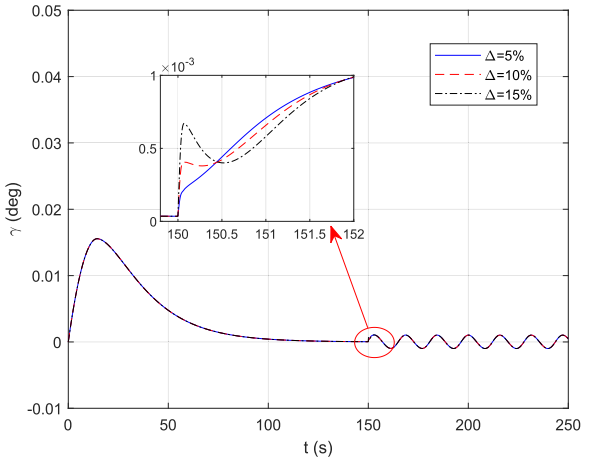

FIGURE 6. Responses of the flight path angle.

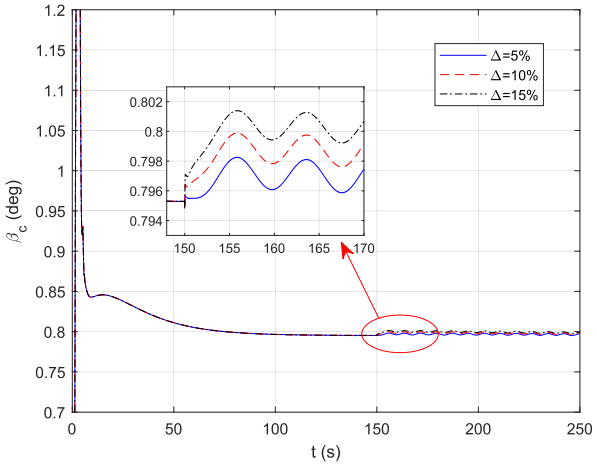

FIGURE 7. Responses of the throttle setting.

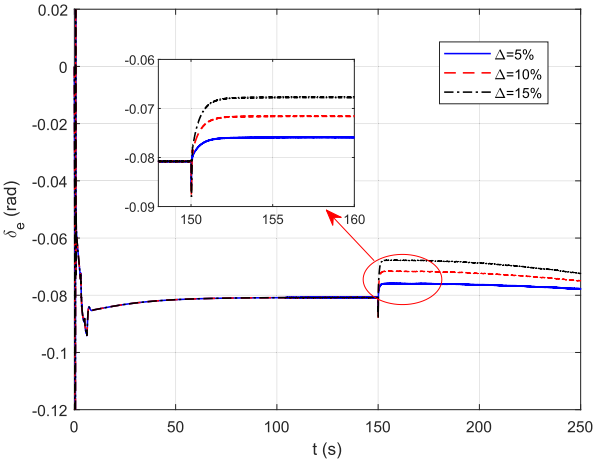

FIGURE 8. Responses of the elevator deflection.

of velocity subsystem and altitude subsystem, respectively. $\Delta = \Lambda\%$ represents the parameter uncertain boundary, it means $\Delta_i = i_0 \cdot \Lambda\% \cdot \sin(\omega t)$, $i = m, s, \bar{c}, c_e, I_{yy}, C_L^{\alpha}, C_D^{\alpha^2}, C_D^{\alpha}, C_D^0, C_T^{\beta}, C_T^0, C_M^{\alpha,\alpha^2}, C_M^{\alpha,\alpha}, C_M^{\alpha,0}, C_M^{q,\alpha^2}, C_M^{q,\alpha}, C_M^{q,0}$. Fig. 3 and Fig. 4 present the tracking performance of altitude and velocity. When the simulation time $t = 150$ (s), both

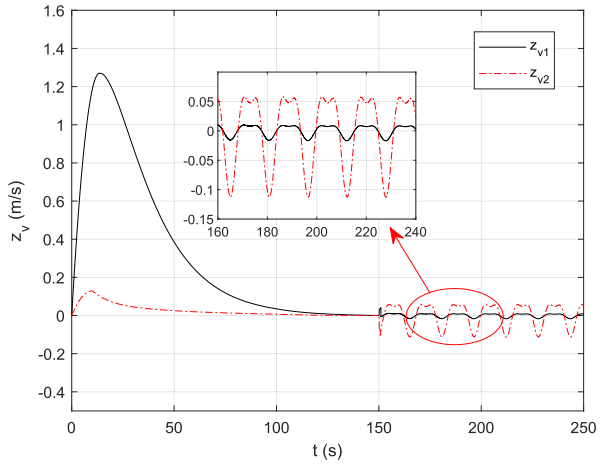

FIGURE 9. Virtual control law of the velocity subsystem.

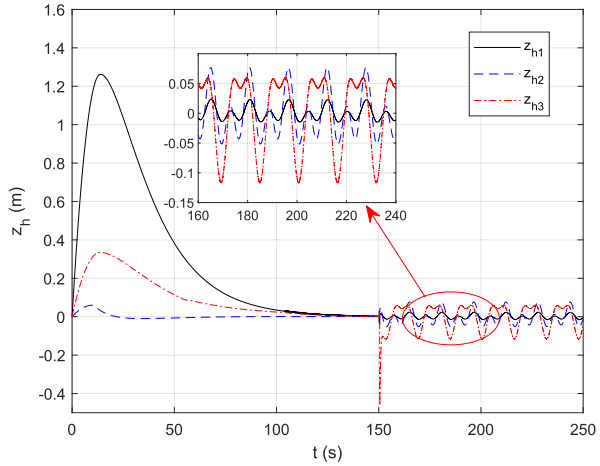

FIGURE 10. Virtual control law of the altitude subsystem.

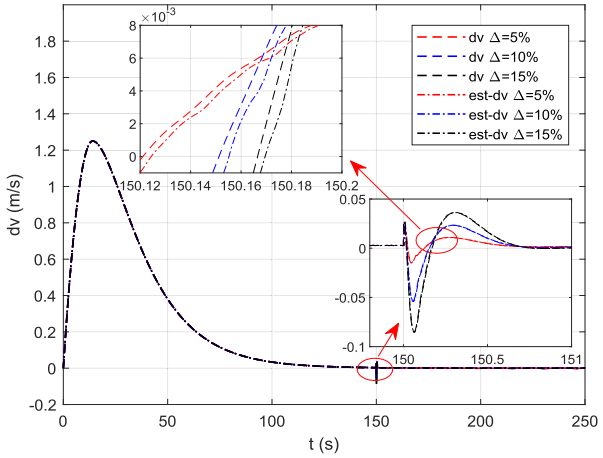

FIGURE 11. Derivative of the velocity.

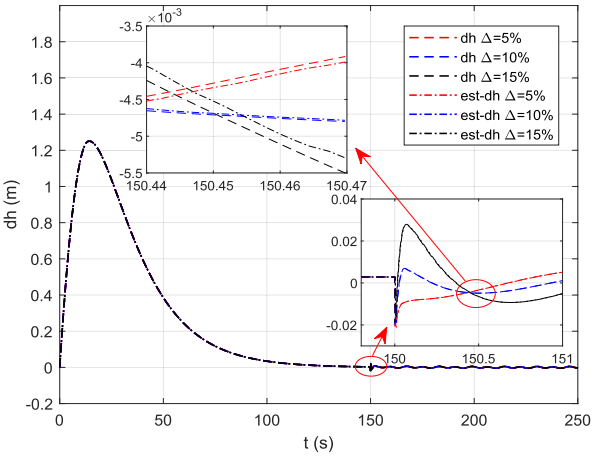

FIGURE 12. Derivative of the altitude.

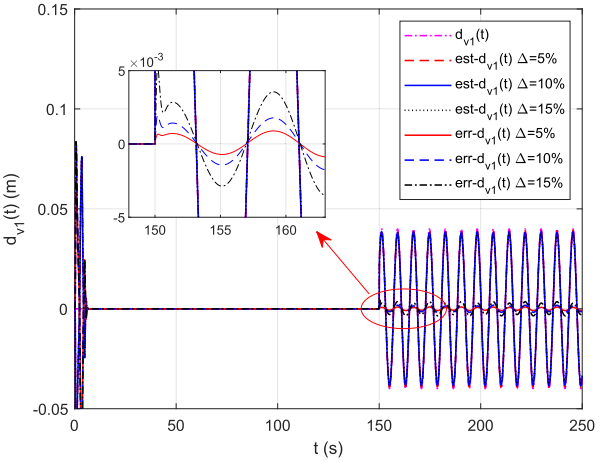

FIGURE 13. Estimations of d_{v_1}.

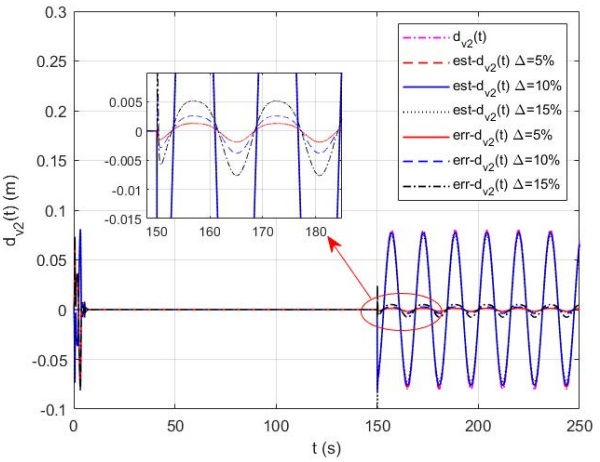

FIGURE 14. Estimations of d_{v_2}.

external disturbances and parameter uncertainties are added to the velocity subsystem and the altitude subsystem. The variations of parameter uncertainties increase from $\Delta = 5\%$ to $\Delta = 15\%$ of their normal values. It can be seen that the closed-loop system is stable, the transient responses of both altitude and velocity are with a smaller fluctuation. After adding parameter uncertainties and external disturbances, the system recovers to stability within 2 seconds. Fig. 5 and

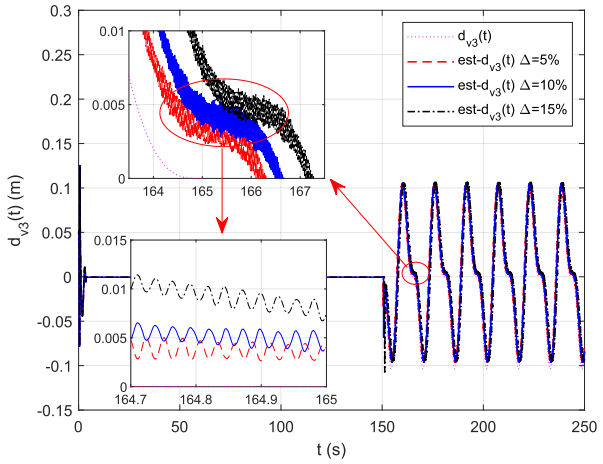

FIGURE 15. Estimations of d_{v_3}.

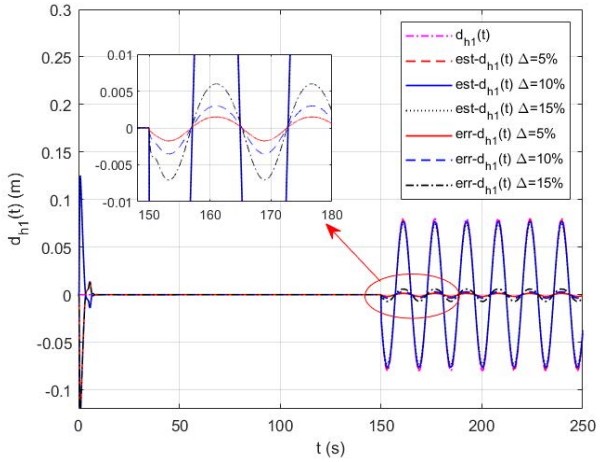

FIGURE 16. Estimations of d_{h_1}.

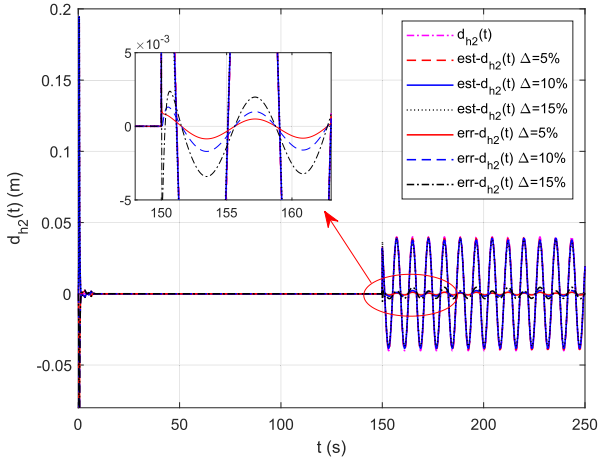

FIGURE 17. Estimations of d_{h_2}.

Fig. 6 are the responses of attack angle and flight path angle; Fig. 7 and Fig. 8 are control inputs of the throttle setting and the elevator deflection. It is shown that the responses of both flight states and control inputs are quite smooth and within

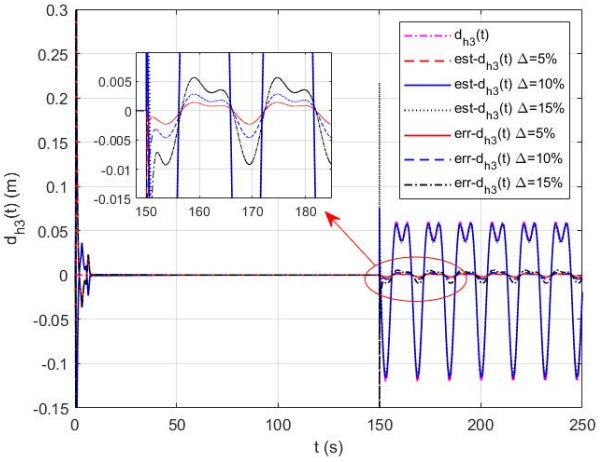

FIGURE 18. Estimations of d_{h_3}.

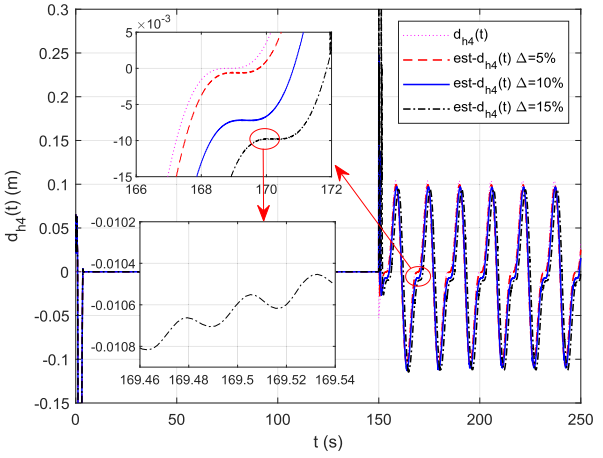

FIGURE 19. Estimations of d_{h_4}.

their rational bounds. The virtual control laws of velocity subsystem and altitude subsystem are depicted in Fig. 9 and Fig. 10, which guarantee that the proposed DSC strategy meet the performance requirements for tracking velocity and altitude reference trajectories.

The estimation performance of the proposed NDO is presented in Figs. 11-19. Fig. 11 and Fig. 12 show that the estimations of the first derivative signal of velocity and altitude under the parameter uncertainties with $\Delta = 5\%$, $\Delta = 10\%$ and $\Delta = 15\%$, respectively. Fig. 13 and Fig. 14 present the estimation performance of velocity subsystem under the external disturbances of d_{v_1} and d_{v_2}. The estimation performance of altitude subsystem under the external disturbances of d_{h_1}, d_{h_2} and d_{h_3} are depicted in Figs. 16-18, respectively. It is observed from Figs. 13-19 that the presented NDO scheme can provide an accurate estimation of external disturbances. The estimation errors of external disturbances of each channel are very small. Fig. 15 and Fig. 19 present the estimation performance of d_{v_3} and d_{h_4}, respectively. It can be seen that the estimation of the velocity subsystem d_{v_3} and the altitude subsystem d_{h_4} translate upward and downward

slightly, respectively. Due to the modeling errors, with the increase of the uncertainty boundary, some uncertain factors have effects on external disturbances, which are within the rational bounds of the estimation performance of NDO. The above simulation analyse show that the presented DSC method can provide a stable tracking of velocity and altitude commands in the presence of external disturbances, owing to the effective estimations of disturbances provided by the developed NDO.

V. CONCLUSION

In this paper, a novel dynamic surface controller (DSC) based on nonlinear disturbance observer (NDO) approach is proposed for air-breathing hypersonic vehicle (AHV) with the mismatched uncertainties and external disturbances. In order to obtain a practical control-oriented model, the longitudinal dynamical model of AHV is described as a strict feedback nonlinear form with mismatched disturbances. In order to solve the problem of ''explosion of terms'', a new tracking differentiator (TD) based on inverse hyperbolic sine function is designed for each step virtual control laws. For the sake of enhancing the robustness of system by estimating and compensating the model uncertainties and disturbances, a new NDO based on the proposed TD is designed for AHV. Simulation results demonstrate that the proposed DSC control method can provide a stable tracking of velocity and altitude commands in the presence of mismatched uncertainties and external disturbances.

In the future work, we will keep on improving the tracking control performance of AHV flight controller. And other forms of control method will be also taken into consideration, such as intelligent control, adaptive control, and sliding mode control, etc.

REFERENCES

[1] C. Zhang, D. Hu, L. Ye, W. Li, and D. Liu, ''Review of the development of hypersonic vehicle technology Abroad in 2017,'' *Tactical Missile Technol.*, vol. 39, no. 1, pp. 47–50, Oct. 2018.
[2] H. An, Q. Wu, G. Wang, Y. Kao, and C. Wang, ''Adaptive compound control of air-breathing hypersonic vehicles,'' *IEEE Trans. Aerosp. Electron. Syst.*, vol. 56, no. 6, pp. 4519–4532, Dec. 2020.
[3] J. Sun, Z. Pu, J. Yi, and Z. Liu, ''Fixed-time control with uncertainty and measurement noise suppression for hypersonic vehicles via augmented sliding mode observers,'' *IEEE Trans. Ind. Informat.*, vol. 16, no. 2, pp. 1192–1203, Feb. 2020.
[4] J. Wang, Q. Zong, R. Su, and B. Tian, ''Continuous high order sliding mode controller design for a flexible air-breathing hypersonic vehicle,'' *ISA Trans.*, vol. 53, no. 3, pp. 690–698, May 2014.
[5] J. Wang, Y. Wu, and X. Dong, ''Recursive terminal sliding mode control for hypersonic flight vehicle with sliding mode disturbance observer,'' *Nonlinear Dyn.*, vol. 81, no. 3, pp. 1489–1510, Aug. 2015.
[6] H. An, Q. Wu, and C. Wang, ''Differentiator based full-envelope adaptive control of air-breathing hypersonic vehicles,'' *Aerosp. Sci. Technol.*, vols. 82–83, pp. 312–322, Nov. 2018, doi: 10.1016/j.ast.2018.09.032.
[7] H. An, H. Xia, and C. Wang, ''Barrier Lyapunov function-based adaptive control for hypersonic flight vehicles,'' *Nonlinear Dyn.*, vol. 88, no. 3, pp. 1833–1853, Jan. 2017.
[8] H. An, Q. Wu, C. Wang, and X. Cao, ''Scramjet operation guaranteed longitudinal control of air-breathing hypersonic vehicles,'' *IEEE/ASME Trans. Mechatronics*, vol. 25, no. 6, pp. 2587–2598, Dec. 2020.
[9] Z. Guo, J. Guo, J. Zhou, and J. Chang, ''Robust tracking for hypersonic reentry vehicles via disturbance estimation-triggered control,'' *IEEE Trans. Aerosp. Electron. Syst.*, vol. 56, no. 2, pp. 1279–1289, Apr. 2020.
[10] Y. Yang, X. Shao, Y. Shi, and W. Zhang, ''Back-stepping robust control for flexible air-breathing hypersonic vehicle via α-filter-based uncertainty and disturbance estimator,'' *Int. J. Control, Autom. Syst.*, vol. 19, pp. 753–766, 2021, doi: 10.1007/s12555-019-1034-0.
[11] J. Farrell, M. Sharma, and M. Polycarpou, ''Backstepping-based flight control with adaptive function approximation,'' *J. Guid. Control Dyn.*, vol. 28, no. 6, pp. 1089–1102, Nov. 2005.
[12] S. Bouabdallah and R. Siegwart, ''Backstepping and sliding-mode techniques applied to an indoor micro quadrotor,'' in *Proc. IEEE Int. Conf. Robot. Autom. (ICRA)*, Barcelona, Spain, Apr. 2005, pp. 2247–2252.
[13] R. Fierro and F. L. Lewis, ''Control of a nonholonomic mobile robot using neural networks,'' *IEEE Trans. Neural Netw.*, vol. 9, no. 4, pp. 589–600, Jul. 1998.
[14] C. Yu, J. Jiang, Z. Zhen, A. K. Bhatia, and S. Wang, ''Adaptive backstepping control for air-breathing hypersonic vehicle subject to mismatched uncertainties,'' *Aerosp. Sci. Technol.*, vol. 107, Dec. 2020, Art. no. 106244, doi: 10.1016/j.ast.2020.106244.
[15] D. Wang and J. Huang, ''Neural network-based adaptive dynamic surface control for a class of uncertain nonlinear systems in strict-feedback form,'' *IEEE Trans. Neural Netw.*, vol. 16, no. 1, pp. 195–202, Jan. 2005.
[16] D. Gao, Z. Sun, and T. Du, ''Dynamic surface control for hypersonic aircraft using fuzzy logic system,'' in *Proc. IEEE Int. Conf. Autom. Logistics*, Jinan, China, Aug. 2007, pp. 2314–2319.
[17] X. Bu, X. Wu, M. Zhen, and Z. Rui, ''Nonsingular direct neural control of air-breathing hypersonic vehicle via back-stepping,'' *Neurocomputing*, vol. 153, pp. 164–173, Apr. 2015.
[18] B. Xu, D. Wang, Y. Zhang, and Z. Shi, ''DOB-based neural control of flexible hypersonic flight vehicle considering wind effects,'' *IEEE Trans. Ind. Electron.*, vol. 64, no. 11, pp. 8676–8685, Nov. 2017.
[19] X. Bu, G. He, and K. Wang, ''Tracking control of air-breathing hypersonic vehicles with non-affine dynamics via improved neural back-stepping design,'' *ISA Trans.*, vol. 75, pp. 88–100, Apr. 2018.
[20] X. Bu, ''Air-breathing hypersonic vehicles funnel control using neural approximation of non-affine dynamics,'' *IEEE/ASME Trans. Mechatronics*, vol. 23, no. 5, pp. 2099–2108, Sep. 2018.
[21] X. Bu, Q. Qi, and B. Jiang, ''A simplified finite-time fuzzy neural controller with prescribed performance applied to waverider aircraft,'' *IEEE Trans. Fuzzy Syst.*, vol. 30, no. 7, pp. 2529–2537, Jun. 2021, doi: 10.1109/TFUZZ.2021.3089031.
[22] X. Bu, B. Jiang, and H. Lei, ''Non-fragile quantitative prescribed performance control of waverider vehicles with actuator saturation,'' *IEEE Trans. Aerosp. Electron. Syst.*, early access, pp. 1–1, Feb. 2022, doi: 10.1109/TAES.2022.3153429.
[23] D. Swaroop, J. K. Hedrick, P. P. Yip, and J. C. Gerdes, ''Dynamic surface control for a class of nonlinear systems,'' *IEEE Trans. Autom. Control*, vol. 45, no. 10, pp. 1893–1899, Oct. 2002.
[24] W. A. Butt, L. Yan, and A. S. Kendrick, ''Robust adaptive dynamic surface control of a hypersonic flight vehicle,'' in *Proc. 49th IEEE Conf. Decis. Control (CDC)*, Atlanta, GA, USA, Dec. 2002, pp. 1893–1899.
[25] W. A. Butt, L. Yan, and A. S. Kendrick, ''Adaptive dynamic surface control of a hypersonic flight vehicle with improved tracking,'' *Asian J. Control*, vol. 15, no. 2, pp. 594–605, Oct. 2013.
[26] X.-W. Bu, X.-Y. Wu, Y.-X. Chen, and R.-Y. Bai, ''Design of a class of new nonlinear disturbance observers based on tracking differentiators for uncertain dynamic systems,'' *Int. J. Control Automat. Syst.*, vol. 13, no. 3, pp. 595–602, Mar. 2015.
[27] X. Bu, X. Wu, R. Zhang, Z. Ma, and J. Huang, ''Tracking differentiator design for the robust backstepping control of a flexible air-breathing hypersonic vehicle,'' *J. Franklin Inst.*, vol. 352, no. 4, pp. 1739–1765, Sep. 2016.
[28] H. An, J. Liu, C. Wang, and L. Wu, ''Approximate back-stepping fault-tolerant control of the flexible air-breathing hypersonic vehicle,'' *IEEE/ASME Trans. Mechatronics*, vol. 21, no. 3, pp. 1680–1691, Jun. 2016.
[29] X. Yin, B. Wang, L. Liu, and Y. Wang, ''Disturbance observer-based gain adaptation high-order sliding mode control of hypersonic vehicles,'' *Aerosp. Sci. Technol.*, vol. 89, pp. 19–30, Jun. 2019.
[30] X. Jiao, B. Fidan, J. Jiang, and M. Kamel, ''Adaptive mode switching of hypersonic morphing aircraft based on type-2 TSK fuzzy sliding mode control,'' *Sci. China Inf. Sci.*, vol. 58, no. 7, pp. 1–15, Jul. 2015.
[31] M. A. Bolender and D. B. Doman, ''Nonlinear longitudinal dynamical model of an air-breathing hypersonic vehicle,'' *J. Spacecraft Rockets*, vol. 44, no. 2, pp. 374–387, Mar. 2007.

OUXUN LI received the B.Sc. and M.Sc. degrees from Chongqing University, Chongqing, China, in 2005 and 2009, respectively. He is currently pursuing the Ph.D. degree with the College of Automation Engineering, Nanjing University of Aeronautics and Astronautics, Nanjing, China. He is a Lecturer with the School of Electronic Information and Automation, Guilin University of Aerospace Technology, China. His research interests include guidance and control of hypersonic vehicle, sliding mode control, auto disturbance rejection control, and backstepping control.

JU JIANG received the B.Sc. degree in flight control and the M.Sc. degree in navigation, guidance and control from Beihang University, Beijing, China, in 1985 and 1987, respectively, and the Ph.D. degree in machine learning and intelligent control from the University of Waterloo, Waterloo, Canada, in 2007. He is currently a Professor with the College of Automation Engineering, Nanjing University of Aeronautics and Astronautics, Nanjing, China. His research interests include guidance and control of shipboard aircraft, large airliner, hypersonic vehicle and unmanned aerial vehicle, machine learning and intelligent control, and nonlinear control.

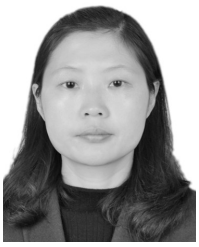

LI DENG received the B.Sc. and M.Sc. degrees from Southwest University, Chongqing, China, in 2005 and 2008, respectively, and the Ph.D. degree from the University of Electronic Science and Technology of China, in 2021. She is currently an Associate Professor with the School of Electronic Information and Automation, Guilin University of Aerospace Technology, China. Her research interests include information and coding theory, LDPC/protograph codes, and wireless image communication.

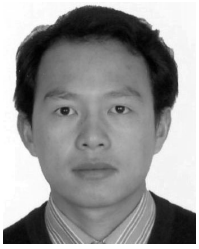

SHUTONG HUANG received the B.Sc. and M.Sc. degrees from Southwest Jiaotong University, Chengdu, China, in 2000 and 2008, respectively. He is currently pursuing the Ph.D. degree with the College of Automation Engineering, Nanjing University of Aeronautics and Astronautics, Nanjing, China. He is a Lecturer with the School of Electronic Information and Automation, Guilin University of Aerospace Technology, China. His research interests include guidance and control of hypersonic vehicle, sliding mode control, and fuzzy logic control.